CLM-P79

United Kingdom Atomic Energy Authority

RESEARCH GROUP

Preprint

FINITE RESISTIVITY INSTABILITIES OF A SHEET PINCH

J. WESSON

Culham Laboratory,

Culham, Abingdon, Berkshire

1965

UNCLASSIFIED
(Approved for publication)

CLM-P79

FINITE RESISTIVITY INSTABILITIES OF A SHEET PINCH

by

J. Wesson

(Submitted for publication in 'Nuclear Fusion')

ABSTRACT

The finite resistivity instabilities of a sheet pinch are studied by numerical analysis in terms of normal modes. Results are obtained for the tearing, ripple and gravitational modes and their dependence on conductivity, wavelength, the gravitational field, the position of $\underline{k} \cdot \underline{B} = 0$ and the position of the walls. Comparison is made with the results of Furth, Killeen and Rosenbluth[1].

U.K.A.E.A. Research Group,
Culham Laboratory,
Nr. Abingdon,
Berks.

June, 1965. (C/18 MEA)

CONTENTS

		Page
1.	INTRODUCTION	1
2.	THE BASIC EQUATIONS	1
3.	METHOD	2
4.	RESULTS	3
5.	ACKNOWLEDGEMENTS	7
6.	REFERENCES	7

1. INTRODUCTION

A sheet pinch with zero resistivity and no gravitational field is hydromagnetically stable. With finite resistivity instabilities are possible and these have been analysed by Furth, Killeen and Rosenbluth (F.K.R.) [1]. The types of instability found are:-

(i) the tearing instability in which the sheet breaks up into separate pinches

(ii) the rippling instability in which a displacement in the region of a resistivity gradient changes the current density by changing the local resistivity.

If a gravitational field in the opposite direction to the density gradient is present, then for zero resistivity the pinch is still stable if the magnetic shear is sufficiently high. If the resistivity is finite the plasma is always unstable.

In the analysis of F.K.R. the problem is treated by dividing the plasma into two regions, a narrow inner region around the plane for which the wave vector is perpendicular to the magnetic field $(\underline{k} \cdot \underline{B} = 0)$, and an outer region in which the finiteness of the resistivity was neglected. In the present work the same basic equations are used but they are solved numerically without any division into separate regions or other approximation. In the model the conductivity has the form as $(1 + (y/a)^2)^{-1}$ about the mid-plane $y = o$ for the study of the tearing and rippling modes and is constant for the gravitational mode.

The variation of growth rate with conductivity, instability wavelength, position of $\underline{k} \cdot \underline{B} = 0$, position of the walls and with gravitational field has been calculated. The eigenfunctions have also been obtained and some are presented here.

2. THE BASIC EQUATIONS

The plasma lies between perfectly conducting walls at $y = \pm y_w$. The magnetic field $\underline{B}\ (B_x, 0, B_z)$ is a function of y only. The basic equations given below are identical with those of F.K.R.

$$\underline{\nabla} \times \left[\rho \frac{d\underline{v}}{dt} - \frac{1}{4\pi} (\underline{\nabla} \times \underline{B}) \times \underline{B} + \rho \underline{g} \right] = 0 \qquad \ldots (1)$$

$$\frac{\partial \underline{B}}{\partial t} = \underline{\nabla} \times \left[\underline{v} \times \underline{B} - \frac{\eta}{4\pi} \underline{\nabla} \times \underline{B} \right] \qquad \ldots (2)$$

$$\left(\frac{\partial}{\partial t} + \underline{v} \cdot \underline{\nabla}\right) \eta = 0 \qquad \ldots (3)$$

$$\left(\frac{\partial}{\partial t} + \underline{v} \cdot \underline{\nabla}\right) (\rho \underline{g}) = 0 \qquad \ldots (4)$$

$$\underline{\nabla} \cdot \underline{v} = 0 \qquad \ldots (5)$$

$$\underline{\nabla} \cdot \underline{B} = 0 \qquad \ldots (6)$$

ρ is the mass density and $\underline{g}$ the gravitational acceleration, the resistivity η and the gravitational force density $\rho\underline{g}$ are assumed to be convected with the plasma.

Linearising and taking Fourier components of the form $\exp(\omega t + i(k_x x + k_z z))$ the equations written in dimensionless variables reduce to

$$\Psi'' = (\alpha^2 + p\tilde{\eta})\,\Psi + HW \qquad \ldots (7)$$

$$W'' = \alpha^2 \left(1 - \frac{S^2}{p^2}(G - pFH)\right) W + \alpha^2 S^2 H\Psi \qquad \ldots (8)$$

where

$$\Psi = B_y/B_s, \quad W = -iv_y k\tau_R,$$

$$F = (\underline{k} \cdot \underline{B})/kB_s, \quad H = (F + \tilde{\eta}' F'/p)\tilde{\eta},$$

$$\alpha = ka, \quad \tau_R = 4\pi a^2/\langle\eta\rangle, \quad \tau_H = a(4\pi\rho)^{\frac{1}{2}}/B_s,$$

$$S = \tau_R/\tau_H, \quad p = \omega\tau_R, \quad \tilde{\eta} = \eta_o/\langle\eta\rangle, \quad G = -\tau_H^2(g/\rho)\frac{\partial\rho}{\partial y}$$

and y has been replaced by a dimensionless variable $Y = y/a$. The constants B_s and $\langle\eta\rangle$ are measures of the magnetic field and resistivity. η_o is the unperturbed resistivity and ρ is the unperturbed density whose gradient is assumed negligible except in as far as it introduces G. It has been assumed that the velocity is zero in the unperturbed state so that $\nabla \times (\eta j) = 0$ and therefore $(\eta F')' = 0$. As will be seen below 'a' is a measure of the thickness of the current layer.

In the present calculation two forms of the conductivity $\sigma\ (= 1/\tilde{\eta})$ and the magnetic field distribution will be considered,

(i) $\sigma = (1 + Y^2)^{-1}$, $F(Y) = \tan^{-1} Y + F(0)$ for $G = 0$

(ii) σ = constant, $F(Y) = Y$ for finite G.

The problem then is to solve equations (7) and (8) for Ψ and W and the eigenvalue p subject to the chosen boundary conditions which are $\Psi = W = 0$ at $Y = \pm Y_w$. It has been shown by F.K.R. that p will be real for unstable perturbations.

3. METHOD

A set of fourth order difference equations is formed from equations (7) and (8). The boundary conditions $\Psi = W = 0$ at $Y = -Y_w$ and $W = 0$ at $Y = +Y_w$ are used and Ψ

is normalized at some point. For the symmetric modes a half range calculation was used with $\Psi' = 0$ and $W = 0$ at $Y = 0$ as the boundary condition. With a trial value p_t of p the value of $\Psi\ (+ Y_w)$ is calculated using Gauss' method. p_t is then varied to reduce $\Psi\ (+ Y_w)$ to a sufficiently small value. The step length is then reduced until the change in p is negligible. For the resulting value of p, Ψ and W are then calculated.

4. RESULTS

In the study of the tearing and ripple modes the conductivity variation and field configuration of type (i) is used.

SYMMETRIC TEARING MODE

This is the case $G = 0$ and $F(0) = 0$. In general the growth rate is a function of α and Y_w and a diagram of the results for $S = 10^3$ is shown in Fig.1. It should be noted that the unit in which Y_w is measured is the characteristic width of the current layer. For any position of the walls there is an upper limit to the wavelength for stability. The limiting value can be determined from the equation for neighbouring equilibria, that is the linearised part of $\underline{\nabla} \times (\underline{j} \times \underline{B}) = 0$. This amounts to finding the eigenvalue α of

$$\Psi'' = (\alpha^2 + \frac{F''}{F})\ \Psi \qquad \ldots (9)$$

with $\Psi = 0$ at $Y = \pm Y_w$. There is also a maximum separation of the walls for stability given by solving equation (9) for Y_w with $\alpha = 0$. As $Y_w \to \infty$ the $p(\alpha)$ profile becomes independent of Y_w, the maximum value of p being 14.67, this value occurring at $\alpha = 0.219$.

EFFECT OF THE POSITION OF $F = 0$

As the position of $F = 0$, which will be called Y_s, moves away from $Y = 0$ the resistivity gradient becomes significant and the unstable mode changes from tearing to ripple for long wavelengths and for short wavelengths instability is introduced by the ripple mode.

This is illustrated in Fig.2 which shows the results for $G = 0$, $Y_w = 10$ and $S = 10^3$. For the long wavelengths ($\alpha = 0.1$) p falls monstonically as Y_s increases, for short wavelengths ($\alpha = 10$) the growth rate is zero for $Y_s = 0$ and reaches a maximum at Y_s just greater than 1.

The change in the eigenfunctions Ψ and W is shown in Figs.3 and 4. Fig.3 is for

the symmetric tearing mode and it is seen that Ψ is symmetric and W is antisymmetric. In Fig.4 $Y_s = -1$ and the displacement is now very non-symmetric.

VARIATION WITH WAVELENGTH

In this section we shall consider the variation of growth rate with wavelength. This is shown in Fig.5 for the case $G = 0$, $Y_w = 10$, $S = 10^3$ and $Y_s = -1$. At $Y = 1$, $\sigma\ (= \tilde{\eta}^{-1}) = \sigma' = \frac{1}{2}$. The upper curve corresponds to the first eigenvalue and the lower to the second. For $\alpha \ll 1$ the tearing effect dominates and the displacement extends over a large part of the plasma as is seen in Fig.4 for $\alpha = 0.1$. As α increases the resistivity gradient effect becomes important and the displacement is more localised. This is illustrated at Fig.6 for $\alpha = 1$. For very large α the growth rate approaches a constant value and the second eigenvalue approaches this value also.

It is interesting at this point to make a comparison with the predictions of F.K.R. The eigenvalue Λ arising in their analysis is defined by

$$\Lambda = \Lambda_1 - \Lambda_2$$

where

$$\Lambda_1 = (\tilde{\eta}')^2/16\ \varepsilon^2\ p^2$$

$$\Lambda_2 = \alpha^2\ \varepsilon^2$$

and

$$\varepsilon = [p\ \tilde{\eta}/4\ \alpha^2\ S^2\ (F')^2]^{\frac{1}{4}}$$

The calculated values of these quantities are shown in Fig.7. For very large α the quantity $\Lambda \to \frac{1}{2}$ and as Λ_1, and Λ_2 are much greater than $\frac{1}{2}$ and increase with α we have $\Lambda_1/\Lambda_2 \to 1$. This corresponds to the case $\alpha^2\ \varepsilon^2 \gg 1$, that is to wavelengths much less than the decoupled layer thickness. As α is decreased $\alpha^2\ \varepsilon^2$ becomes negligible and Λ falls to a value much less than $\frac{1}{2}$. This is in complete agreement with F.K.R. theory.

However according to the F.K.R. assumption that the decoupled layer is much smaller than the thickness of the plasma layer, that is $\varepsilon \ll 1$, Λ would approach zero as α approaches zero whereas it is seen that for sufficiently small α, ε becomes comparable with and then greater than 1 and Λ then rises to a high value.

VARIATION WITH CONDUCTIVITY

A plot of the variation of the dimensionless growth rate p against S is given in

Fig.8 for $G = 0$, $Y_w = 10$, $Y_s = -1$ and $\alpha = 1$. S is proportional to the conductivity of the plasma. It is seen that p increases with S, it should be noted however that p is defined in terms of the conductivity and that the actual growth rate decreases with increasing conductivity. The theory of F.K.R. predicts the dependence to be $p \propto S^{2/5}$ A line having this dependence is given in the figure and it is seen that the F.K.R. theory gives the correct form for large S where it is expected to be most accurate.

THE GRAVITATIONAL MODE

For finite G cases the configuration chosen was $F = Y$, that is σ = constant (=1) and $F'' = 0$. The boundary conditions were either $\Psi' = W = 0$ or $\Psi = W' = 0$ at $Y = 0$ and $\Psi = W = 0$ at $Y = Y_w$. In this case it is possible to remove one parameter by rewriting equations (7) and (8) in the form

$$\frac{d^2\tilde{\Psi}}{dX^2} = (Q + E)\,\tilde{\Psi} + Q\,X\,\tilde{W}$$

and

$$\frac{d^2\tilde{W}}{dX^2} = \left(E - \frac{G}{Q^2} + \frac{X^2}{Q}\right)\tilde{W} + \frac{X}{Q}\tilde{\Psi}$$

where $E = (\alpha^2/S)^{2/3}$, $Q = p/(S^2E)^{1/2}$, $X = (S^2E)^{1/4}Y$, $\tilde{\Psi} = (S^2E)^{1/4}\Psi$ and $\tilde{W} = W/p$. However the numerical results obtained are presented in terms of the original variables for clarity and for consistency with the previous sections. The results may be applied to conditions other than those stated by use of the above relations.

It was found that the variation of the growth rate with Y_w was in general small for $Y_w > 1$ and Y_w was put equal to 1 except where otherwise stated.

Fig.9 shows the variation of p with S for the symmetric mode for $\alpha = 10$ and $G = 0.1$ and 1.0. For this model, but with perfect conductivity, the Suydam criterion is $G > \frac{1}{4}$. For low G F.K.R. found that $p \propto S^{2/3}$ and for high G, $p \propto S$. The present results give almost straight lines in the logarithmic plot and the slopes give $p \propto S^{0.74}$ for $G = 0.1$ and $p \propto S^{0.81}$ for $G = 1.0$. It appears that in the range of values studied $p \propto S^{\upsilon}$ is a good approximation where υ is some function of G.

The variation of p with G for the symmetric Ψ mode is given by curve 1 in Fig.10 for $\alpha = 10$ and $S = 10^3$. It is compa ed with the results of F.K.R. which for this case give

$$p = (S\,\alpha\,G/2\Lambda)^{2/3} \qquad G \ll \tfrac{1}{4} \qquad \text{curve 2}$$

$$P = S\,[G - (G - \tfrac{1}{2})^{1/2}]^{1/2} \qquad G \gg \tfrac{1}{2} \qquad \text{curve 3.}$$

The correct value for Λ is slightly less than 3/2 and curve 2 is plotted with $\Lambda = 3/2$. It is seen that there is good agreement in the high and low G limits.

Fig.11 shows the variation of p with α for $S = 10^3$ and $G = 0.1$ and 1.0 for both the symmetric and the antisymmetric modes. For these cases Y_w was put equal to 20 principally to remove the effect of the walls for high G and low α. The F.K.R. theory gives $p \propto \alpha^{2/3}$ for low G and p independent of α for large G provided $\alpha \gg 1$. The rates of variation of p for the cases given falls between these as expected, the high G case having the slower variation with α. For small G the eigenvalues of the symmetric and antisymmetric modes are degenerate as $\alpha \to 0$[2] and the approach of the eigenvalues is apparent in the case $G = 0.1$.

DISCUSSION

From the results described above it is seen that the solution of the fourth order equation gives results which overall are in general agreement with the "boundary layer" calculation of F.K.R. and which are in precise agreement in the appropriate limiting cases. It is of interest therefore to use the numerical results to discuss the approximations made by F.K.R.

The basic assumption of F.K.R. is that the plasma may be divided into regions. In the narrow inner region around $\underline{k} \cdot \underline{B} = 0$, $\eta \underline{j}$ is not negligible and it is necessary to use the fourth order equation. In the outer region the inertial term in the equation of motion is negligible and $\underline{E} + \underline{v} \times \underline{B} \simeq 0$ so that the perturbations may be obtained by solving a second order equation (equation 9) which is independent of p. A second assumption which is used is that Ψ is constant over the region where the $\eta \underline{j}$ term is important.

The eigenfunctions for the symmetric case $G = 0$, $Y_w = 10$, $S = 10^3$, $\alpha = 0.1$ are shown in Fig.3. In Fig.12 the inner region is shown with the solution Ψ_o of the outer region equation $\nabla \times (\underline{j} \times \underline{B}) = 0$, that is equation (9), and also the value of W obtained using $\underline{E} + \underline{v} \times \underline{B} = 0$, that is $W_o = -\frac{P}{F} \Psi$ where Ψ has the value obtained using the fourth order equation. It is seen that the assumption that equation (9) holds in an outer region is valid and $\underline{E} + \underline{v} \times \underline{B} = 0$ in this region.

Equation (9) has been used to obtain the value of $\Delta' = (\Psi'/\Psi)_2 - (\Psi'/\Psi)_1$ where the suffices refer to the values on either side of the point $F = 0$. For the case under consideration the F.K.R. theory gives $p = (\sqrt{2}\, \alpha S \Delta'/3)^{4/5}$ and for $\alpha = 0.1$, $S = 10^3$ the value of Δ' has been computed to be 8.434 giving $p = 19.04$. The computed value of p

is 11.99. The reason for this discrepancy is clear from Fig.12 where it is seen that Ψ varies considerably over the region where the approximation $\underline{E} + \underline{v} \times \underline{B} = 0$ is invalid.

The above situation may be contrasted with the case where $\alpha = 0.5$ but the other conditions are unchanged. Fig.13 gives the solution in the inner region. It is seen that Ψ varies only slightly in this region where $\underline{E} + \underline{v} \times \underline{B} = 0$ is invalid. The value of p using the F.K.R. approximation is now 12.22 and the correct value is 10.55 which is considerably better agreement than in the previous case.

5. ACKNOWLEDGEMENTS

The author would like to thank Mr. G. Bernau and Miss D. Drogman for writing the programme used in the calculations presented here and Miss Drogman for her help in assembling the numerical results.

6. REFERENCES

1. FURTH, H.P., KILLEEN, J. and ROSENBLUTH, M.N. Physics of Fluids 6 (1963) 459.

2. JOHNSON, J.L., GREENE, J.M. and COPPI, B. Physics of Fluids 6 (1963) 1169.

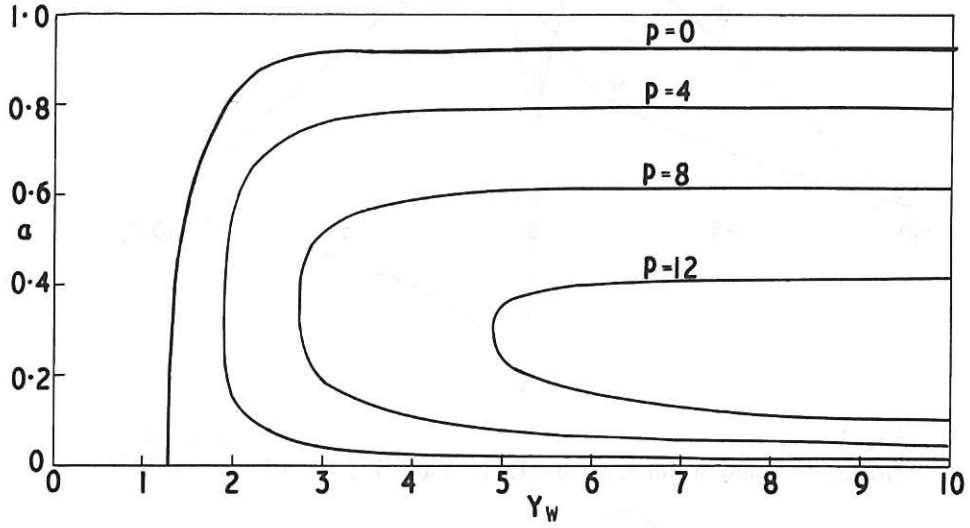

Fig. 1 (CLM-P79)
Symmetric tearing mode. Contours of constant ρ in the a, Y_W plane for $S = 10^3$

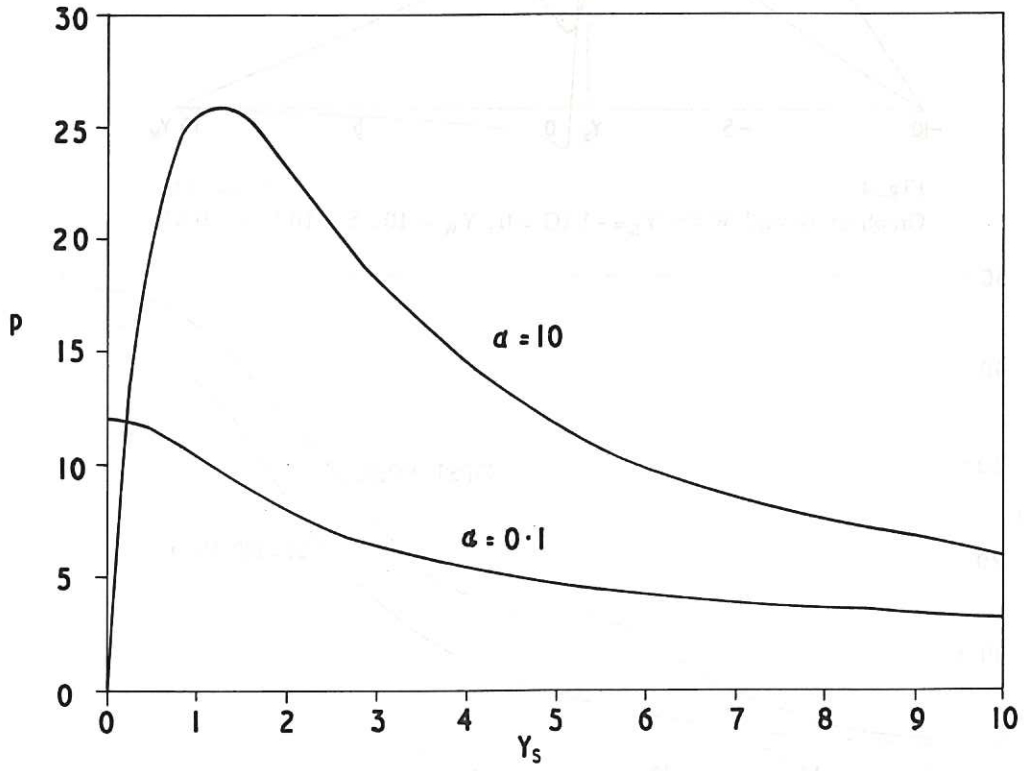

Fig. 2 (CLM-P79)
Variation of p with Y_S for $a = 0.1$ and $a = 10$ ($G = 0$, $Y_W = 10$, $S = 10^3$)

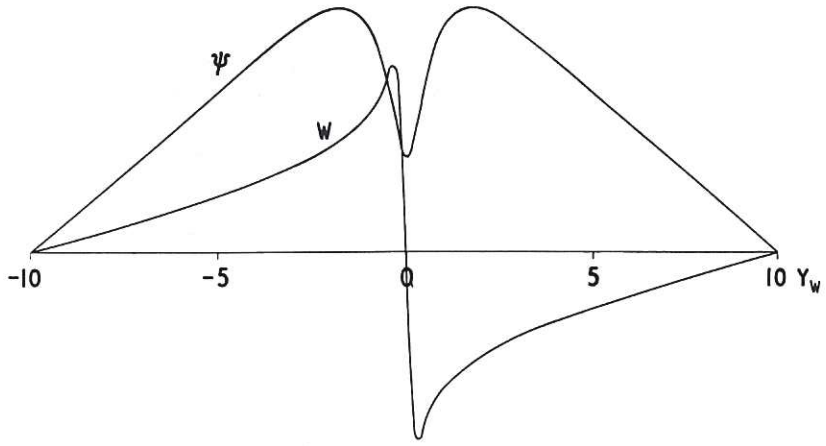

Fig. 3 (CLM-P79)
Graph of ψ and W for $Y_S = 0$ ($G = 0$, $Y_W = 10$, $S = 10^3$, $\alpha = 0.1$)

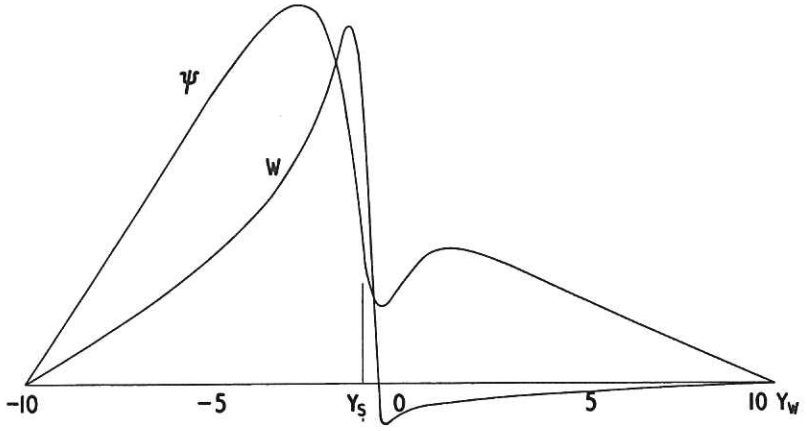

Fig. 4 (CLM-P79)
Graph of ψ and W for $Y_S = -1$ ($G = 0$, $Y_W = 10$, $S = 10^3$, $\alpha = 0.1$)

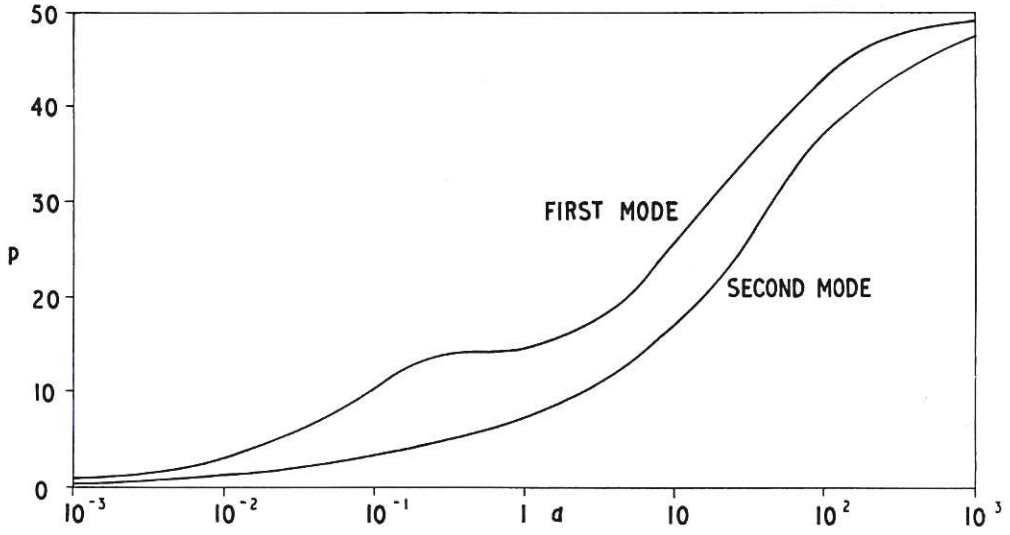

Fig. 5 (CLM-P79)
Graph of growth rate p against wavelength α for first and second Eigenmodes ($G = 0$, $Y_W = 10$, $Y_S = -1$, $S = 10^3$)

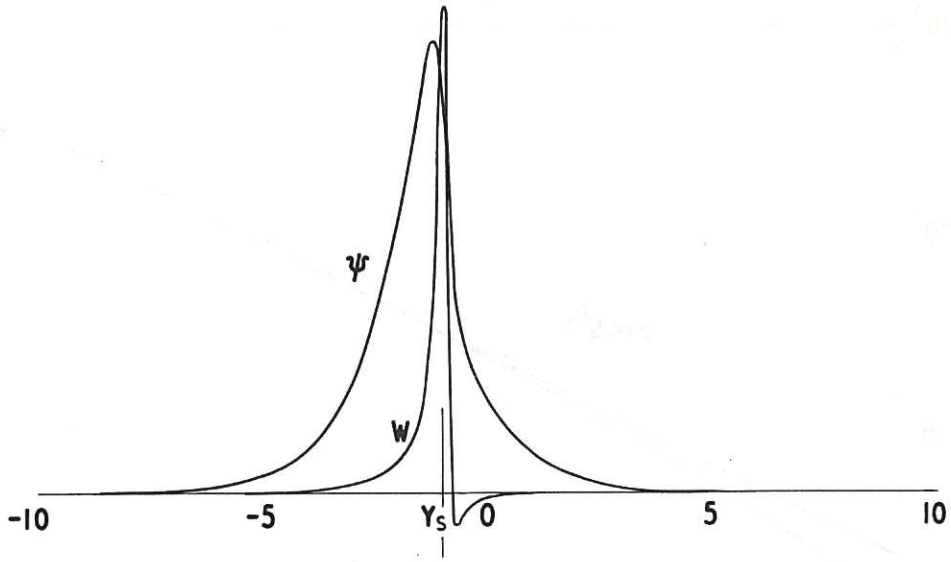

Fig. 6 (CLM-P79)
Graph of ψ and W for $\alpha = 1.0$ ($G = 0$, $Y_W = 10$, $Y_S = -1$, $S = 10^3$)

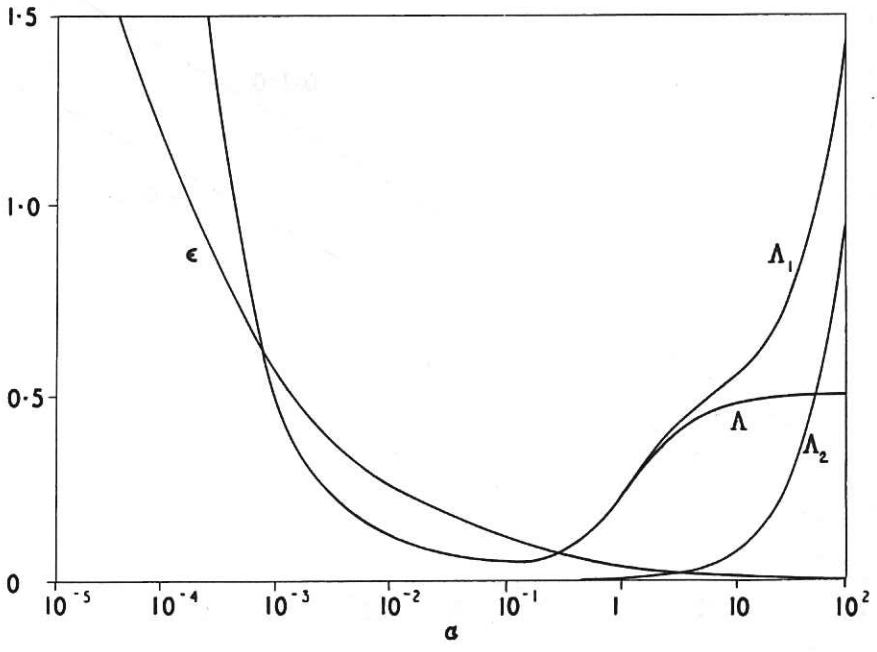

Fig. 7 (CLM-P79)
Graphs of Λ_1, Λ_2, Λ and ϵ as function of α ($G=0$, $Y_W=10$, $S=10^3$, $Y_S=-1$)

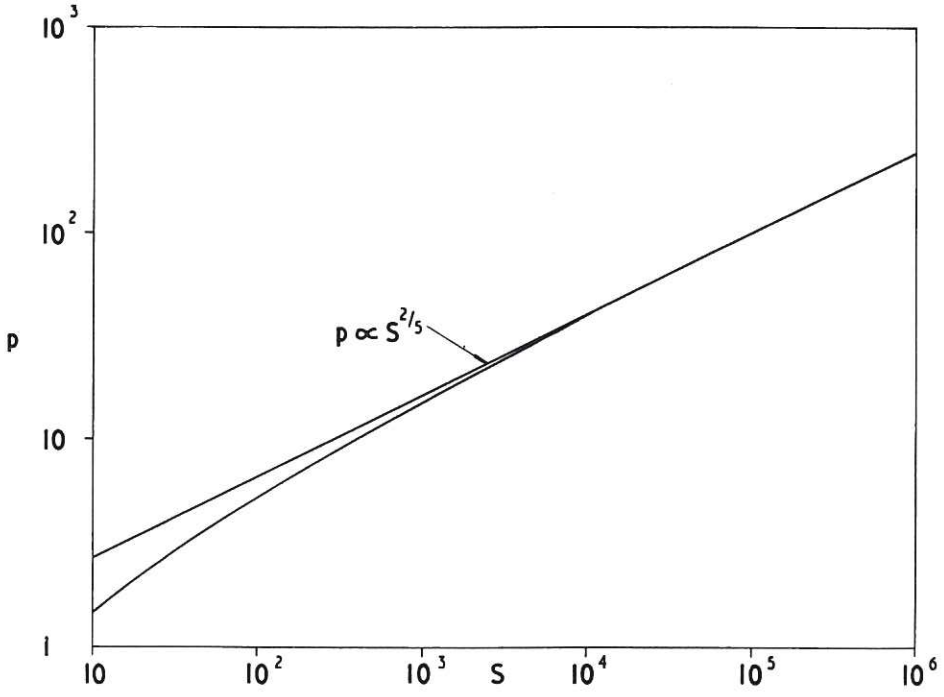

Fig. 8 (CLM-P 79)
Graph of p against S ($G = 0$, $Y_W = 10$, $Y_S = -1$, $\alpha = 1$)

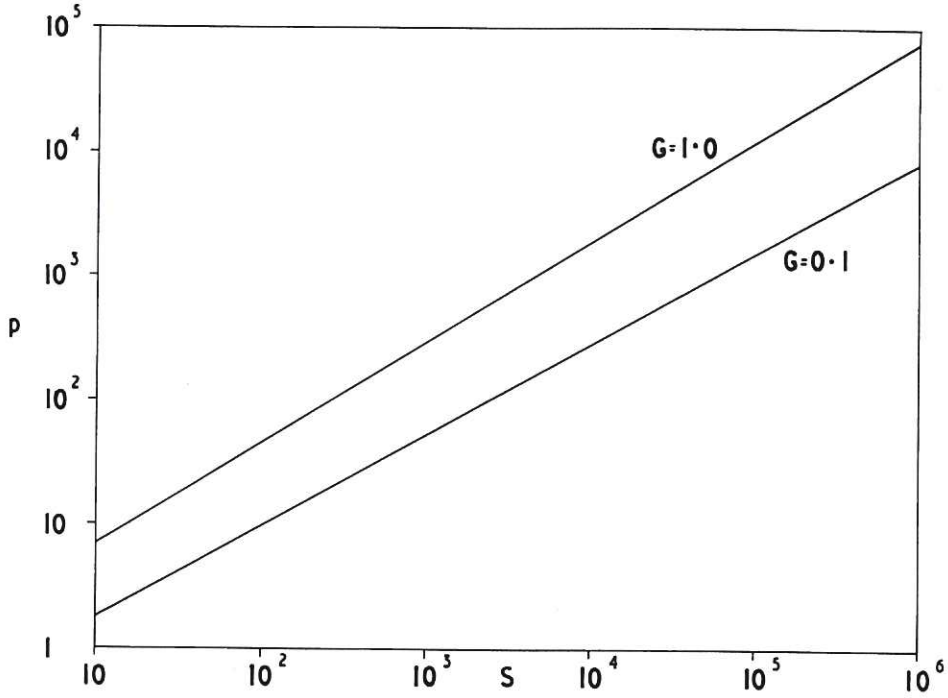

Fig. 9 (CLM-P 79)
Plot of p against S for $G = 0.1$ and $G = 1.0$ with $\alpha = 10$

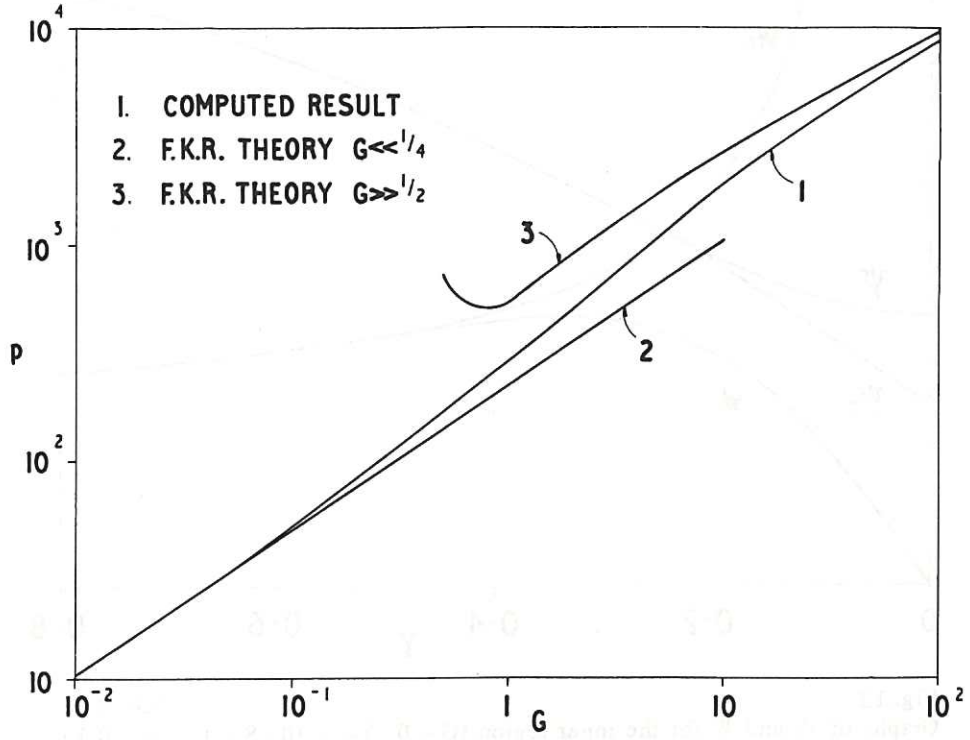

Fig. 10 (CLM-P79)
Graphs of p against G ($\alpha = 10$, $S = 10^3$)

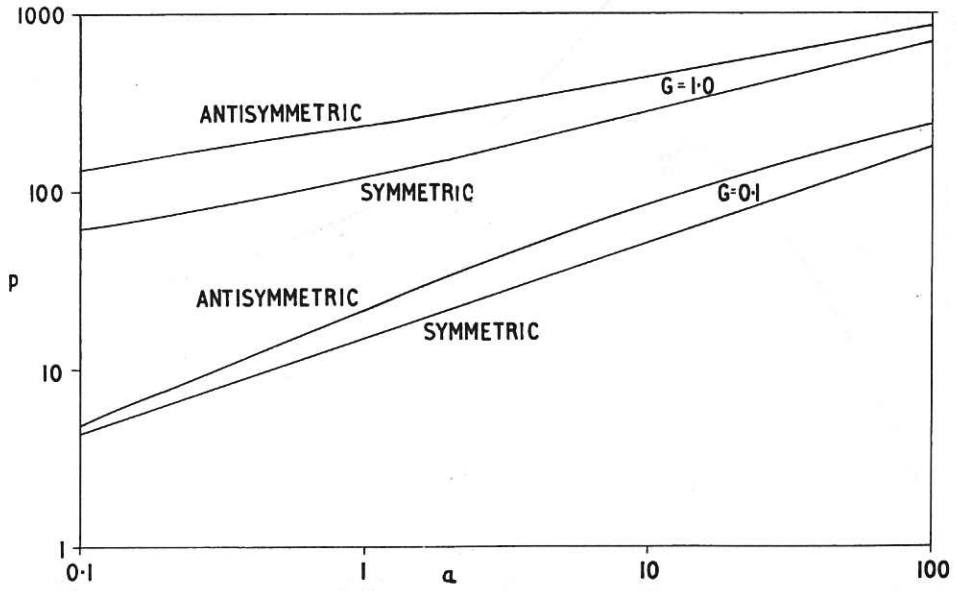

Fig. 11 (CLM-P79)
Graphs of p against α for G = 0.1 and G = 1.0 with $S = 10^3$

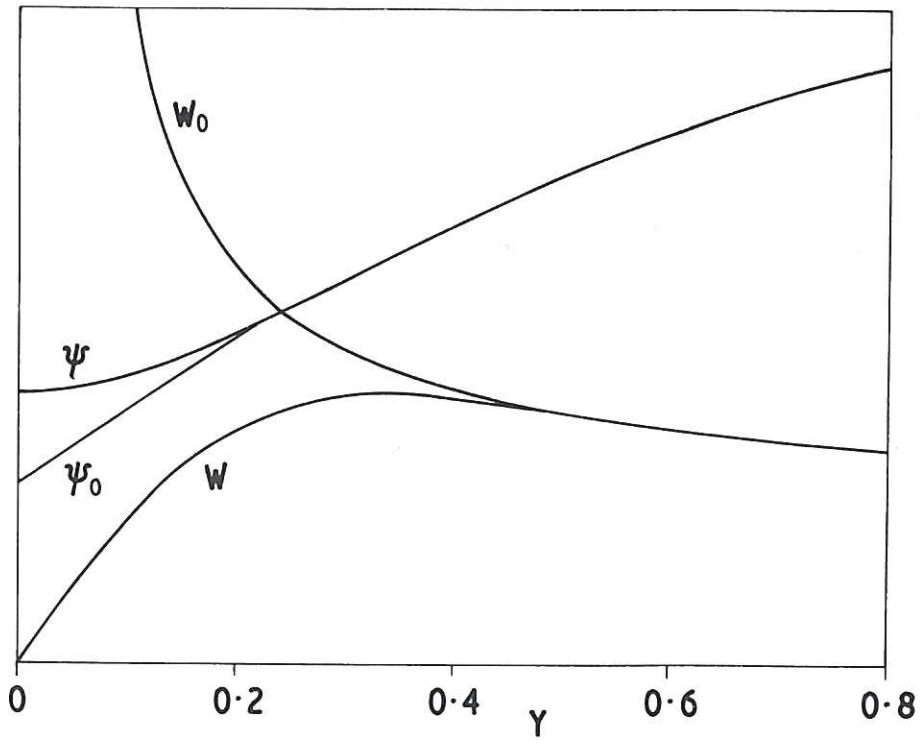

Fig. 12 (CLM-P79)
Graphs of ψ and W for the inner region ($G = 0$, $Y_W = 10$, $S = 10^3$, $\alpha = 0.1$)

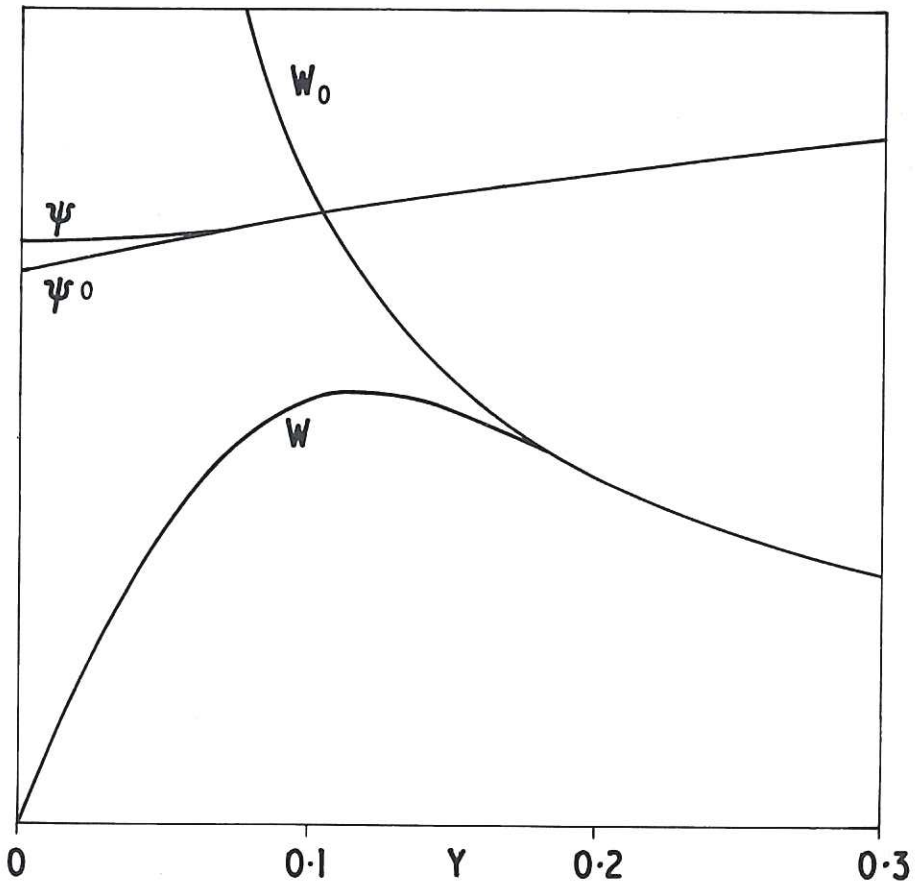

Fig. 13 (CLM-P79)
Graphs of ψ and W for the inner region ($G = 0$, $Y_W = 10$, $S = 10^3$, $\alpha = 0.5$)